Multi-GHz femtosecond pulses from linear and non-linear propagation of a phase-modulated laser

HANYU YE[1,*], LILIA PONTAGNIER[1], ERIC CORMIER[1,2], AND GIORGIO SANTARELLI[1]

[1] Laboratoire Photonique Numérique et Nanosciences (LP2N), UMR 5298, CNRS-IOGS-Université Bordeaux, 33400 Talence, France
[2] Institut Universitaire de France (IUF),1 rue Descartes, 75231 Paris, France
[*] Corresponding author: hanyu.ye@institutoptique.fr

Compiled August 15, 2022

We propose and demonstrate a non-mode-locking approach to generating multi-GHz repetition rate, femtosecond pulses in burst mode by shaping a continuous-wave (CW) seed laser in an all-fiber configuration. The seed laser at 1030 nm is first phase modulated and dechirped to low-contrast, ∼2 ps pulses at 17.5 GHz repetition rate, then carved to bursts at 60 kHz repetition rate, and finally shaped to sub-2 ps clean pulses by a Mamyshev regenerator. This prepared high-quality picosecond source is further used to seed a Yb-doped fiber amplifier operating in the highly nonlinear regime, delivering output pulses at 23 nJ/pulse and 20 μJ/burst, compressible to ∼100 fs level. The system eliminates the need of mode-locked cavities and simplifies conventional ultrafast electro-optic combs to using only one phase modulator, while providing femtosecond pulses at multiple GHz repetition rate, enhanced pulse energy in burst mode and the potential of further power/energy scaling.

http://dx.doi.org/10.1364/ao.XX.XXXXXX

Ultrashort laser pulse generation at GHz repetition rate has attracted more and more attention in recent years. With tens or hundreds of times higher repetition rate, GHz lasers are advantageous compared to conventional MHz-repetition-rate, mode-locked lasers in many areas, such as high-efficiency laser ablation [1], real-time spectroscopy [2], high-speed optical transmission systems [3] and frequency-comb related applications where accessing individual comb lines is necessary [4–6]. In recent years, by pushing the limit of cavity lengths, researchers have achieved mode locking with multiple GHz pulse repetition rates [7–10]. However, these ultrashort cavities limit the gain and make the self-starting mode locking become challenging. Besides, the large free spectral ranges of these multi-GHz repetition rate lasers give each longitudinal mode proportionally larger linewidths, heavily raising their phase noise, which could be undesirable for further frequency comb applications. As an alternative, electro-optic (EO) frequency combs, being intensively developed these years, represent an alternative way of generating ultrashort pulses at multi-GHz repetition rates free of mode locking [11–14]. Driven by a radio-frequency (RF) signal, EO combs offer an all-fiber configuration with widely tunable and accurate repetition rate setting, up or down quasi-linear chirp for convenient pulse compression, narrow comb lines and possible stabilization of the carrier-envelope offset frequency depending on the seed laser.

Ultrafast EO combs are usually composed of a continuous-wave (CW) seed laser, a few phase modulators (2 or 3) to broaden the spectrum, an intensity modulator to carve pulses and various RF electronics. Simplifying the high-power EO part to a simple phase modulator could greatly reduce the complexity and cost. However, this limits the spectral bandwidth and results in low pulse contrast after compression [15]. In optical communication community, it has been demonstrated that Mamyshev regenerators based on self-phase modulation (SPM) and spectral filtering can effectively tailor such low-contrast pulses and remove their temporal pedestals, leading to clean picosecond output [16–18]. However, the use of 0.5-1 km of special highly nonlinear fibers designed for telecommunication band for generating SPM doesn't represent a universal approach for developing high-power ultrafast fiber lasers. At ∼1 μm wavelength, spectral masking of such a simple phase-modulated EO comb also enabled clean 9 ps pulses at 20 GHz repetition rate [19]. These pulses are further nonlinearly compressed down to 190 fs, however, using two separate stages involving dissipative free-space optics and critical power injected into 56 m of dispersion-decreasing photonic crystal fiber for soliton compression. To date, the potential of these simple phase-only modulated EO combs for developing all-fiber femtosecond lasers with scalable output power/energy, as a non-mode-locking approach, hasn't been explored. In this letter, we demonstrate a multi-GHz repetition-rate, femtosecond laser system, realized by nonlinearly shaping and amplifying a phase-only modulated EO comb at 1030 nm in an all-standard-fiber configuration. In the first step, we transform the CW seed laser to clean sub-2 ps pulses at 17.5 GHz repetition rate by phase-modulation, pre-compression, burst shaping and Mamyshev regeneration. In the second step, we further amplify these shaped picosecond pulses in a fiber amplifier to 1.2 W output power, corresponding to 23 nJ/pulse and 20 μJ/burst. The use of burst mode facilitates nonlinear pulse shaping through a Mamyshev regenerator and enables the final fiber amplifier to operate in the deep nonlinear regime, leading to output pulses compressible down to ∼100 fs level.

The experimental setup for the burst-mode, all-fiber laser

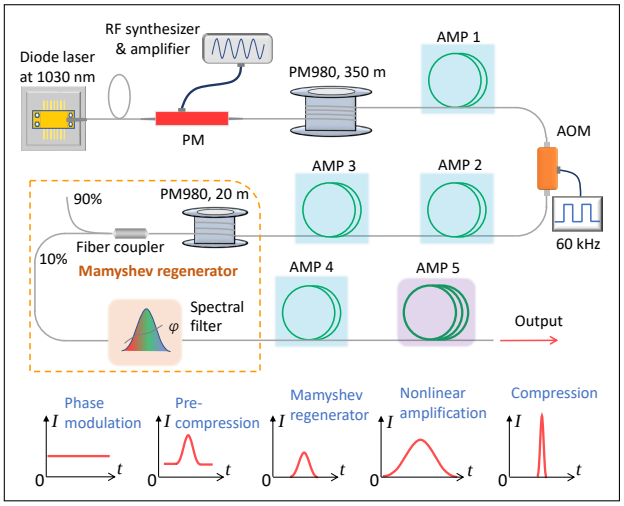

Fig. 1. Experimental setup for the 17.5 GHz, burst-mode femtosecond laser system and illustration of its pulse evolution. PM, phase modulator; AMP, amplifier; AOM, acousto-optic modulator.

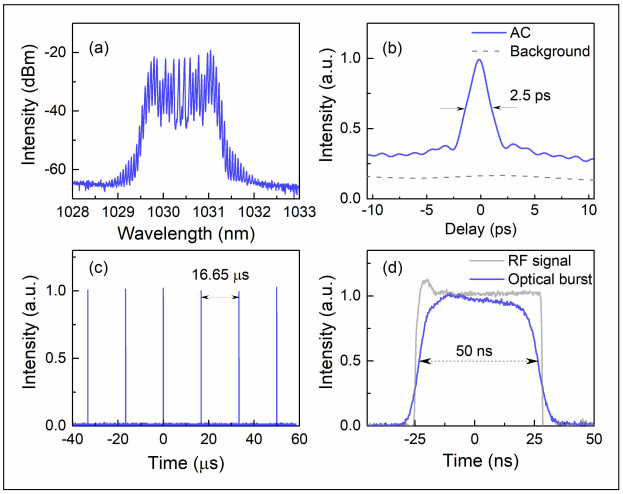

Fig. 2. Measured (a) spectrum and (b) autocorrelation of the phase-modulated EO comb. Measured (c) burst train at 60 kHz repetition rate and (d) temporal profile of optical bursts with their driving RF signal.

system at 17.5 GHz repetition rate based on a phase-only modulated EO comb is depicted in Fig. 1. The EO comb consists of a CW single-frequency diode laser at 1030 nm and an EO phase modulator driven by an amplified RF signal at 17.5 GHz, featuring greatly reduced complexity and cost, compared to a conventional version [11]. The sinusoidal modulation of the laser phase broadens the seed laser's spectrum with comb lines evenly spaced by 17.5 GHz and, at the same time, introduces quasi-linear up and down chirps. The quasi-linear down chirp is then compensated in 350 m of standard polarization-maintaining fiber (PM980), leading to the compression of the modulated photons associated with the down chirp, while the photons modulated with the opposite chirp acquire an additional chirp further extending their temporal span, resulting in a significant pedestal and a limited overall pulse. We further linearly amplify the formed pulses using a core-pumped, Yb-doped fiber amplifier (YDFA, 6/125 μm) and send them into an acousto-optic modulator (AOM) to produce bursts. The AOM is driven by a square RF wave, yielding output bursts of 50 ns at 60 kHz repetition rate. The isolated pulse number per burst is ~880 and the reduced pulse number per second is ~53 million, corresponding to a duty cycle of 0.3%. To compensate the power loss in the AOM, we use two stages of core-pumped, YDFA (6/125 μm) to boost the power to 220 mW. At this point, the intra-burst pulses are still sitting on a pedestal, limiting their temporal contrast. To tackle this limitation, we employ a Mamyshev regenerator, consisting of 20 m of PM980 fiber and a programmable pulse and spectrum shaper (Finisar, 1000S). The PM980 fiber, as a nonlinear medium, broadens the input spectrum by SPM and optical wave-breaking, while the pulse shaper works as a spectral band-pass filter which is centered away from the input spectrum. As such, the transmitted spectrum through the filter only comes from nonlinear broadening of the input pulses and the low-intensity temporal pedestal located at input spectral band is blocked. In the experiment, by setting the spectral filter as a Gaussian shape centered at either 1024 nm or 1037 nm, we manage to extract clean picosecond pulses free of pedestal. Note that a 10% fiber coupler is used prior to the pulse shaper only for avoiding damage.

After Mamyshev regeneration, we use another core-pumped YDFA similar to above as a pre-amplifier and a cladding-pumped YDFA (10/125 μm) as the final amplifier. In this final stage, we combine 3 mW seed pulses with a multi-mode pump laser at 915 nm and inject them into a 3.7 m long Yb-fiber (Coherent, PLMA-YDF-10/125-VIII). This relatively long length compensates the low pump absorption and allows the input pulses to evolve through the parabolic shaping gradually into a newly discovered regime where the spectrum continuously broadens toward longer wavelengths due to SPM and the evolving gain spectrum along the active fiber [20–22]. The amplified pulses are finally extracted from residual pump by a dichroic mirror and compressed by a grating-pair compressor with a groove density of 300 lines/mm. The whole process of pulse shaping in this all-fiber laser system is also illustrated in Fig. 1.

We start the characterization of the laser system from the phase modulated seed laser. Figure 2(a) displays the EO comb spectrum after phase-only modulation with resolved comb lines spaced by 17.5 GHz. The spectrum has a square profile with a 3 dB width of 1.3 nm. Compared to a conventional ultrafast EO comb, the spectrum here shows a less smooth profile with a few missing comb lines due to the lack of an intensity modulator. In the temporal domain, the compressed pulses by 350 m of PM980 fiber at 17.5 GHz repetition rate were also characterized by autocorrelation (AC). The AC trace, as shown in Fig. 2(b) has a full-width-at-half-maximum (FWHM) duration of 2.5 ps, implying a pulse duration around 2 ps. However, the far wings of the AC trace are significantly lifted above the background level, indicating these initial compressed pulses sit on a CW pedestal. Before shaping the pulses, we first carve them into bursts to improve the pulse energy and facilitate the following nonlinear spectral broadening. The optical bursts were characterized by using an oscilloscope with a bandwidth of 1.5 GHz and a fast photodiode with a bandwidth of 40 GHz. The measured bursts, as shown in Fig. 2(c), are evenly separated by 16.7 μs, corresponding to 60 kHz repetition rate. Their temporal profile is also measured, having a duration of ~50 ns, as displayed in Fig. 2(d). The leading and trailing edges of the optical bursts are less sharp than the driving RF signal, limited by the response time of the AOM.

With much enhanced pulse energy in the burst mode, we achieved nonlinear pulse cleaning through a Mamyshev regenerator. The spectrum of the input pulses for the regenerator was first broadened by SPM and optical wave-breaking in the single-mode fiber, then band-pass filtered by a Gaussian shape of ∼1 nm width. The spectra before and after filtering are both shown in Fig. 3. In the broadened spectrum, there are four smooth lobes available for filtering, located around 1024 nm, 1027.5 nm, 1033 nm and 1035-1040 nm, respectively. However, the two in the middle are too close to the original EO comb spectrum, so that a Gaussian filter at these two wavelengths can not completely suppress the input spectral peak and thus the temporal pedestal. Besides, these two spectral lobes have narrower bandwidths and less flat profiles, which would result in narrow spectrum and longer pulses after filtering. In the experiment, we performed spectral filtering at both 1024 nm and 1037 nm, and let the two filtered spectra have similar 3 dB bandwidths of 1.05 nm and 0.9 nm, respectively.

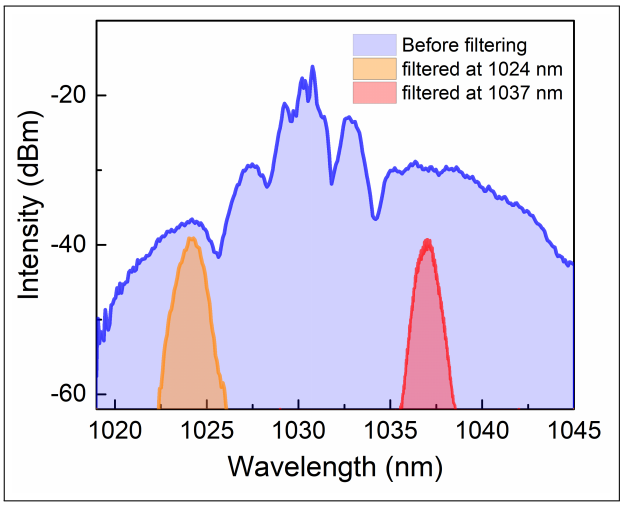

Fig. 3. Measured spectra after broadening and filtering in the Mamyshev regenerator.

Although other simple thin-film interference spectral filters can be used, here we use a programmable pulse shaper as the filter which not only allows us to shape the spectrum, but also provides tunable dispersion to compress the filtered pulses. As such, we can obtain clean picosecond pulses near Fourier-transform (FT) limit for further nonlinear amplification. At the output of the Mamyshev regenerator, we used a short core-pumped YDFA where the amplification is kept as a linear process. Then we measured the AC traces of the shaped pulses, as shown in Fig. 4(a) and (b). By providing -0.85 ps^2 group delay dispersion, the shaped pulses were de-chirped to 1.6 ps at 1024 nm and 1.8 ps at 1037 nm, assuming a Gaussian fit. Their time-bandwidth products are calculated to be 0.48 and 0.45. Different from the AC of the initial compressed pulses in Fig. 2(b), the AC traces here have clean profiles free of CW pedestal at far wings, confirming the effectiveness of the Mamyshev regenerator.

Last, we sent these shaped sub-2 ps pulses into the final cladding-pumped YDFA by fusion splicing and performed nonlinear amplification. With a relatively high optical gain of ∼26 dB, we boosted the seed power up to 1.2 W, corresponding to 23 nJ/pulse and 20 μJ/burst. Pumping the amplifier at 915 nm allows a uniform gain distribution along the active fiber and the lower absorption coefficient than at 976 nm helps reduce amplified spontaneous emission. The amplified output pulses were further compressed by using a pair of diffraction gratings. In order to avoid large third-order dispersion distorting ultrashort pulses, we used two transmission gratings with a groove density of 300/mm, arranged at Littrow angle. In the experiment, we first amplified the shaped pulses at 1037 nm. The measured output spectrum at 1.2 W is shown in Fig. 5(a). The input pulses trigger SPM as they propagate and grow along the active fiber, and finally develop a broadband output spectrum with a narrow peak at the input wavelength. The evolving gain spectrum along the active fiber continuously shifts to longer wavelengths upon propagation, which explains the asymmetric spectral shape extending above 1080 nm. Figure 5(b) displays the AC trace of the compressed output pulses as well as the calculated FT limited AC trace based on the measured spectrum for comparison. The measured AC duration is 165 fs while it is 105 fs at FT limit. Compared to the FT limited AC trace, the measured one shows slowly decaying tails, implying residual high-order dispersion in the compressed pulses.

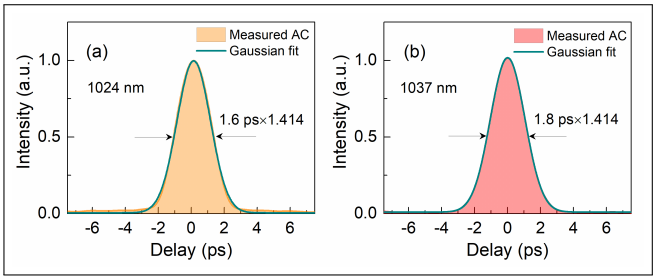

Fig. 4. Measured autocorrelation traces of the shaped pulses by the Mamyshev regenerator at (a) 1024 nm and (b) 1037 nm.

Furthermore, we also performed nonlinear amplification of the shaped pulses at 1024 nm. At the same output power of 1.2 W, we measured the output spectrum which is displayed in Fig. 5(c). Similar to the case in Fig. 5(a), the spectrum is greatly broadened by SPM and the dynamically evolving gain spectrum, having a 10 dB bandwidth of 32 nm. However, we noticed that the center of the spectrum has moved to ∼1037 nm, 11 dB stronger than the spectral intensity at the input wavelength of 1024 nm. This central wavelength shift can be attributed to reabsorption at shorter wavelengths in the Yb-fiber. The smooth spectral peak around 1037 nm should represent the gain center of the active fiber, which coincides with the wavelength of the input pulses in Fig.5(a) and thus explains the narrow spike on the output spectrum when seeding the amplifier at 1037 nm. Fig. 5(d) shows the measured AC trace of the compressed output pulses when using seed pulses at 1024 nm, as well as the calculated AC trace of FT limited pulses. The measured AC trace has a duration of 130 fs, shorter than the case in Fig. 5(b) and close to the calculated AC duration of 102 fs at FT limit. For Gaussian pulses, the deconvoluted pulse duration should be 92 fs for a FT limit of 72 fs. The cleaner AC profile with shorter tails also implies less residual high-order dispersion in the compressed pulses. Having noticed the different performance of the nonlinear fiber amplifier for different seed wavelengths, we further implemented an independent experiment where we used the same fiber amplifier as the nonlinear gain medium and a mode-locked fiber oscillator as the seed. Since the oscillator emits a smooth spectral profile, we could select arbitrary seed wavelengths between 1024 nm and 1038 nm and further study the impact of different seed wavelengths on the amplifier's per-

formance. Relevant results are presented in Supplement 1.

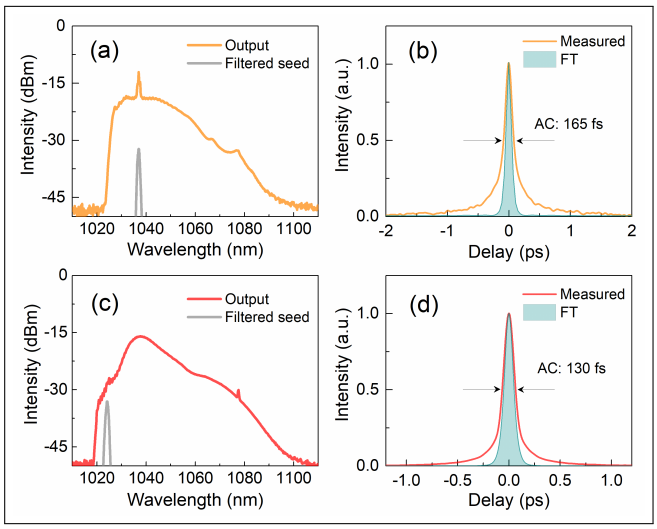

Fig. 5. (a) Measured output spectra of the final amplifier when using seed pulses at (a) 1037 and (c) 1024 nm. Autocorrelation traces of the compressed output pulses when using seed pulses at (b) 1037 nm and (d) 1024 nm.

In conclusion, we have demonstrated a multi-GHz repetition rate, femtosecond fiber laser system in burst mode achieved by phase-only modulating a CW seed laser and further nonlinear propagation. In the first step, the seed laser is phase modulated and pre-compressed to ∼2 ps pulses sitting on a pedestal at 17.5 GHz repetition rate, then carved to bursts of 60 kHz repetition rate, and finally shaped to sub-2 ps clean pulses by a Mamyshev regenerator. In the second step, we further amplify these shaped pulses through a cladding-pumped YDFA, generating 1.2 W output power, corresponding to 23 nJ/pulse and 20 μJ/burst. The burst mode operation significantly improves the pulse energy and facilitates nonlinear pulse shaping through the Mamyshev regenerator. Besides, the enhanced seed pulse energy also enables the final conventional YDFA to operate in the nonlinear regime, leading to output pulses compressible down to ∼100 fs level with seed wavelength optimization. The present laser system proposes a new way of developing multi-GHz repetition rate, energy-enhanced, femtosecond lasers in all-fiber configuration using phase-only modulated EO combs. We believe further power/energy scaling should be naturally feasible when using active fibers with larger mode areas or seeding solid-state amplifiers, which could be of great interest in the fields of high-power laser development and relevant applications, especially advanced material processing with laser bursts.

Funding. Agence Nationale de la Recherche (ANR-10-IDEX-03-02); Institut Universitaire de France; H2020 LEIT Information and Communication Technologies (H2020-ICT-2018); Conseil Régional Nouvelle Aquitaine (2019-1R5M04).

Acknowledgments. The authors acknowledge financial supports from the French National Research Agency (ANR) in the frame of "the investments for the future" Program IdEx Bordeaux – LAPHIA (ANR-10-IDEX-03-02), the Institut Universitaire de France, and European Union's Horizon 2020 research and innovation programme under grant agreement No 825246 (Flexiburst).

Disclosures. The authors declare no conflicts of interest.

Data availability. Data underlying the results presented in this paper are not publicly available at this time but may be obtained from the authors upon reasonable request.

Supplemental document. See Supplement 1 for supporting content.

REFERENCES

1. K.Sugioka, Int. J. Extrem. Manuf. **3**, 043001 (2021).
2. T. Voumard, J. Darvill, T. Wildi, M. Ludwig, C. Mohr, I. Hartl, and T. Herr, Opt. Lett. **47**, 1379 (2022).
3. B. Corcoran, M. Tan, X. Xu, A. Boes, J. Wu, T. G. Nguyen, S. T. Chu, B. E. Little, R. Morandotti, A. Mitchell *et al.*, Nat. Commun. **11**, 1 (2020).
4. S. T. Cundiff and A. M. Weiner, Nat. Photonics **4**, 760 (2010).
5. E. Obrzud, M. Rainer, A. Harutyunyan, B. Chazelas, M. Cecconi, A. Ghedina, E. Molinari, S. Kundermann, S. Lecomte, F. Pepe, F. Wildi, F. Bouchy, and T. Herr, Opt. Express **26**, 34830 (2018).
6. M. Yu, Y. Okawachi, C. Joshi, X. Ji, M. Lipson, and A. L. Gaeta, ACS Photonics **5**, 2780 (2018).
7. A. Barh, B. Özgür Alaydin, J. Heidrich, M. Gaulke, M. Golling, C. R. Phillips, and U. Keller, Opt. Express **30**, 5019 (2022).
8. X. Gao, Z. Zhao, Z. Cong, G. Gao, A. Zhang, H. Guo, G. Yao, and Z. Liu, Opt. Express **29**, 9021 (2021).
9. R. Thapa, D. Nguyen, J. Zong, and A. Chavez-Pirson, Opt. Lett. **39**, 1418 (2014).
10. X. Chen, W. Lin, W. Wang, X. Guan, X. Wen, T. Qiao, X. Wei, and Z. Yang, Opt. Lett. **46**, 1872 (2021).
11. A. Aubourg, J. Lhermite, S. Hocquet, E. Cormier, and G. Santarelli, Opt. Lett. **40**, 5610 (2015).
12. H. Ye, F. Leroi, L. Pontagnier, G. Santarelli, J. Boullet, and E. Cormier, Opt. Express **30**, 10605 (2022).
13. A. Ishizawa, T. Nishikawa, A. Mizutori, H. Takara, H. Nakano, T. Sogawa, A. Takada, and M. Koga, Opt. express **19**, 22402 (2011).
14. D. R. Carlson, D. D. Hickstein, W. Zhang, A. J. Metcalf, F. Quinlan, S. A. Diddams, and S. B. Papp, Science **361**, 1358 (2018).
15. T. Komukai, T. Yamamoto, and S. Kawanishi, IEEE photonics technology letters **17**, 1746 (2005).
16. P. Mamyshev, "All-optical data regeneration based on self-phase modulation effect," in *24th European Conference on Optical Communication. ECOC'98 (IEEE Cat. No. 98TH8398),* , vol. 1 (IEEE, 1998), pp. 475–476.
17. D. Wang, L. Huo, Y. Li, D. Zhang, L. Wang, H. Li, X. Jiang, and C. Lou, Appl. Opt. **57**, 2930 (2018).
18. K. Igarashi and K. Kikuchi, IEEE journal selected topics quantum electronics **14**, 551 (2008).
19. B. Chapman, A. Doronkin, S. Popov, and J. Taylor, Opt. Lett. **37**, 3099 (2012).
20. P. Repgen, D. Wandt, U. Morgner, J. Neumann, and D. Kracht, Opt. Lett. **44**, 5973 (2019).
21. P. Sidorenko, W. Fu, and F. Wise, Optica **6**, 1328 (2019).
22. P. Sidorenko and F. Wise, Opt. Lett. **45**, 4084 (2020).

FULL REFERENCES

1. K.Sugioka, "Will ghz burst mode create a new path to femtosecond laser processing?" Int. J. Extrem. Manuf. **3**, 043001 (2021).
2. T. Voumard, J. Darvill, T. Wildi, M. Ludwig, C. Mohr, I. Hartl, and T. Herr, "1-ghz dual-comb spectrometer with high mutual coherence for fast and broadband measurements," Opt. Lett. **47**, 1379–1382 (2022).
3. B. Corcoran, M. Tan, X. Xu, A. Boes, J. Wu, T. G. Nguyen, S. T. Chu, B. E. Little, R. Morandotti, A. Mitchell *et al.*, "Ultra-dense optical data transmission over standard fibre with a single chip source," Nat. Commun. **11**, 1–7 (2020).
4. S. T. Cundiff and A. M. Weiner, "Optical arbitrary waveform generation," Nat. Photonics **4**, 760–766 (2010).
5. E. Obrzud, M. Rainer, A. Harutyunyan, B. Chazelas, M. Cecconi, A. Ghedina, E. Molinari, S. Kundermann, S. Lecomte, F. Pepe, F. Wildi, F. Bouchy, and T. Herr, "Broadband near-infrared astronomical spectrometer calibration and on-sky validation with an electro-optic laser frequency comb," Opt. Express **26**, 34830–34841 (2018).
6. M. Yu, Y. Okawachi, C. Joshi, X. Ji, M. Lipson, and A. L. Gaeta, "Gas-phase microresonator-based comb spectroscopy without an external pump laser," ACS Photonics **5**, 2780–2785 (2018).
7. A. Barh, B. Özgür Alaydin, J. Heidrich, M. Gaulke, M. Golling, C. R. Phillips, and U. Keller, "High-power low-noise 2-ghz femtosecond laser oscillator at 2.4μm," Opt. Express **30**, 5019–5025 (2022).
8. X. Gao, Z. Zhao, Z. Cong, G. Gao, A. Zhang, H. Guo, G. Yao, and Z. Liu, "Stable 5-ghz fundamental repetition rate passively sesam mode-locked er-doped silica fiber lasers," Opt. Express **29**, 9021–9029 (2021).
9. R. Thapa, D. Nguyen, J. Zong, and A. Chavez-Pirson, "All-fiber fundamentally mode-locked 12 ghz laser oscillator based on an er/yb-doped phosphate glass fiber," Opt. Lett. **39**, 1418–1421 (2014).
10. X. Chen, W. Lin, W. Wang, X. Guan, X. Wen, T. Qiao, X. Wei, and Z. Yang, "High-power femtosecond all-fiber laser system at 1.5 μm with a fundamental repetition rate of 4.9 ghz," Opt. Lett. **46**, 1872–1875 (2021).
11. A. Aubourg, J. Lhermite, S. Hocquet, E. Cormier, and G. Santarelli, "Generation of picosecond laser pulses at 1030 nm with gigahertz range continuously tunable repetition rate," Opt. Lett. **40**, 5610–5613 (2015).
12. H. Ye, F. Leroi, L. Pontagnier, G. Santarelli, J. Boullet, and E. Cormier, "High-power nonlinear amplification of an ultrafast electro-optic frequency comb with flexible ghz repetition rate," Opt. Express **30**, 10605–10613 (2022).
13. A. Ishizawa, T. Nishikawa, A. Mizutori, H. Takara, H. Nakano, T. Sogawa, A. Takada, and M. Koga, "Generation of 120-fs laser pulses at 1-ghz repetition rate derived from continuous wave laser diode," Opt. express **19**, 22402–22409 (2011).
14. D. R. Carlson, D. D. Hickstein, W. Zhang, A. J. Metcalf, F. Quinlan, S. A. Diddams, and S. B. Papp, "Ultrafast electro-optic light with subcycle control," Science **361**, 1358–1363 (2018).
15. T. Komukai, T. Yamamoto, and S. Kawanishi, "Optical pulse generator using phase modulator and linearly chirped fiber bragg gratings," IEEE photonics technology letters **17**, 1746–1748 (2005).
16. P. Mamyshev, "All-optical data regeneration based on self-phase modulation effect," in *24th European Conference on Optical Communication. ECOC'98 (IEEE Cat. No. 98TH8398),* vol. 1 (IEEE, 1998), pp. 475–476.
17. D. Wang, L. Huo, Y. Li, D. Zhang, L. Wang, H. Li, X. Jiang, and C. Lou, "Pedestal-free 25-ghz subpicosecond optical pulse source for 16$\times$ 25-gb/s otdm based on phase modulation and dual-stage nonlinear compression," Appl. Opt. **57**, 2930–2934 (2018).
18. K. Igarashi and K. Kikuchi, "Optical signal processing by phase modulation and subsequent spectral filtering aiming at applications to ultrafast optical communication systems," IEEE journal selected topics quantum electronics **14**, 551–565 (2008).
19. B. Chapman, A. Doronkin, S. Popov, and J. Taylor, "All-fiber integrated 10 ghz repetition rate femtosecond laser source based on raman compression of pulses generated through spectral masking of a phase-modulated diode," Opt. Lett. **37**, 3099–3101 (2012).
20. P. Repgen, D. Wandt, U. Morgner, J. Neumann, and D. Kracht, "Sub-50 fs, μj-level pulses from a mamyshev oscillator–amplifier system," Opt. Lett. **44**, 5973–5976 (2019).
21. P. Sidorenko, W. Fu, and F. Wise, "Nonlinear ultrafast fiber amplifiers beyond the gain-narrowing limit," Optica **6**, 1328–1333 (2019).
22. P. Sidorenko and F. Wise, "Generation of 1 μj and 40 fs pulses from a large mode area gain-managed nonlinear amplifier," Opt. Lett. **45**, 4084–4087 (2020).